DEVELOPMENT OF CORROSION-FREE CONDUCTIVE SUBSTRATES FOR PHOTOVOLTAIC APPLICATIONS TO PORCELAIN TILE USING THE ELECTROLESS PROCESS

[1] M.D. Reyes-Tolosa, [1] M. al Ajami, [1] J. Orozco-Messana, [1] V. Donderis, [1] M.Pascual, [2] M.A. Hernández-Fenollosa

[1] Polytechnic University of Valencia, Instituto de Tecnología de Materiales, Camino de Vera s/n, Valencia (Spain); jaormes@cst.upv.es

[2] Department of Applied Physics, Polytechnic University of Valencia, Cami de Vera s/n, 46071, Valencia, (Spain)

ABSTRACT

In the incipient world of functional industrial ceramics with photovoltaic applications, there is a need to reduce production costs while maximizing the systems' useful life. The thin contact layers currently being manufactured are based on vacuum systems with high production costs and major problems of accelerated corrosion in photovoltaic applications.

The electroless process produces very even and compact layers with very low costs through chelate-based chemicals.

These layers have been formulated in this study with a view to obtaining appropriate electric characteristics for an optimum photoelectric performance in the assemblies. The morphological requirements are previously fitted through a glaze that acts as a barrier layer between the deposited coating and the porcelain tile, applied through tape casting.

The characterisation of the metal layers obtained is started by SEM, an AFM and the Hall effect in order to determine the morphology and chemical characteristics required for these contact layers. The electric characterisation also allows their capacity for offering an optimum performance in the assemblies to be assessed. Finally, the performance of these layers with respect to corrosion is assessed in order to complete the assessment of their industrial suitability.

1. INTRODUCTION

The latest breakthroughs in architectures for solar cells have allowed significant improvements in the performance of these assemblies to be obtained [1]. However, these breakthroughs have led to a tremendous complexity and production cost. The improvement in performance is focused on cell yield, while the cost presupposes increasing the range of substrates and thin-layer deposition techniques in order to control the economic impact of materials and processes.

The wide interest that exists in the ceramic sector in increasing the functionality of tiles in building construction (building-integrated photovoltaics (BIPV)) [2] has led to considering fabrication of photovoltaic modules on commercial ceramic substrates [3]. One single construction element thus supplies the housing with energy and the typical functions of a ceramic envelope. The ceramic envelope used in screens (ventilated façades) allows a very propitious platform to be developed as a photovoltaic materials support due to its high stability, rigidity, modularity and architectural implementation. The ventilated facade concept is especially suitable for assembling this new generation of BIPV modules, since this building solution offers significant saving on the mechanical support of the module tile, and the possibility of special designs, in which wiring and assembly costs are minimised.

The technological development of this family of modules has faced the difficulty of placing a conducting layer between the ceramic substrate and the photovoltaic material which, as well as a charge collector, acts as a barrier layer against the spread of species that damage cell performance and durability. The industrially available technological solutions pose significant difficulties, together with an unacceptable cost for this new family of BIPV modules, which need to compete in price with their limited efficiency.

Contact metallization can be achieved through cathode spraying, evaporation, lithography and electrodeposition. Each of these entails different problems [4], and the high cost is common to all of them.

It is within this facet that the study of economic and reliable layer metallization offers an original solution. This paper presents a functional optimization and characterisation of layer metallization obtained in a mixed form through the electroless deposition of chemical nickel on a layer of the same thermally sprayed metal [5]. The ZnO electrodeposition on these metal layers is being considered as a basis for future hybrid cells with a very low cost.

This article addresses in depth the optimum processing conditions for these layers by studying the influence of polishing on the critical parameters that characterise the application of these layers on industrial porcelain tile.

2. SAMPLE PREPARATION

2.1. Ceramic substrate.

A commercial ceramic product was used that was provided by the firm Ceramicas Belcaire. This is a typical porcelain tile, which was characterised with regard to its chemical composition and dilatometry. In the chemical composition, those atomic species that are dangerous for photovoltaic material were looked for. As shown in the X-ray diffractogram (figure 1), only the presence of sodium was detected. In the dilatometry, the optimum firing temperature (1200ºC) was determined for adjusting the formulation of the glaze that was applied on to the pressed porcelain tile before firing.

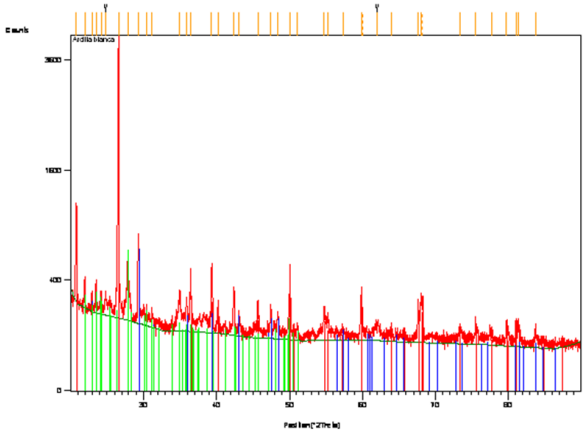

Figure 1. X-ray diffractogram of the raw material for pressing.

The glaze was formulated based on 200-gram batches of suspension. The design objective was focused on obtaining a fluxing glaze with no sodium content and with sufficient percentages of zinc (in the form of ZnO) and titanium dioxide (in the form of anatase) to effectively act as a barrier layer. At the same time, a sintering temperature of over 900ºC has to be reached, with softening at over 1100ºC and fusion in the range of 1270-1300ºC for compatibility with the body. In all the formulations, the following quantities of components for 200 grams of suspension are repeated:

- 120 g powdered glaze.
- 1.6 g dispersant (fish oil).
- 64 g solvent (ethanol with acetone at 50 vol %).
- 10.4 g binding agent (polyvinyl butyral or PVB).
- 4 g plasticiser (benzyl butyl phthalate or BBP).

The glaze powder consisted of ZnO powder (99% purity), anatase (99% purity), quartz, feldspar and alumina. The suspension was ground in a ball mill for one hour for homogenization observing the suppliers' particle sizes. The glaze was then applied on to the pressed substrate using the tape-casting technique

with a green thickness of 2 mm. The final mixture was fired in an industrial kiln at 1200ºC.

2.2. Thermal spraying and polishing.

The fired ceramic samples were subjected to thermal spraying of micro-structured nickel powder (Castodyn 30-40 μm) using a Castodyn DS 10 oxy-acetylene spray gun [6] in order to obtain suitable bonding between the layer to be electrolessly deposited and the ceramic glaze [7].

The samples obtained this way were also subjected to polishing in order to determine the importance of surface polishing on the corrosion performance of the Ni layer and the electric performance of these samples after electrodeposition of ZnO. Polishing was done manually using 1 μm diamond, and automatically (using vibration in a Bruehler Vibromet apparatus) for 3, 6, 9 and 12 hours with 0.25 μm diamond. This was intended to determine the influence of polishing on the performance of these layers. The times and particle sizes selected matched the most representative data in the literature [8].

2.3. Electroless.

The thermally sprayed layers do not have the surface regularity or electric continuity conditions required for making photovoltaic materials grow on them. The ceramic surfaces (with the thermally sprayed nickel) must be catalysed for electroless nickel deposition to be achieved [9]. The formulation for the catalysing ink used consisted of palladium acetate diluted in a 50% solution by volume of Monsanto polymer B70 and isopropyl alcohol. After the samples were immersed in this solution, they were activated in an oven at 300ºC for 24 hours.

All solutions for electroless deposition require [10]: a reducing agent (sodium hydrophosphite), a stabilizer (gluconic acid and sodium tartrate) plus a complexing agent (ammonium hydroxide). Nickel sulphate and molybdenum were used as a source of metal ions (Ni). A ratio of nickel to molybdenum of Ni/Mo = 1.77 was chosen. The molybdenum function is to improve the metal layer resistance to corrosion and to favour nucleation of the ZnO in the electrodeposition stage [5].

The electroless deposition process was carried out at 85ºC for 3 minutes.

2.4. Electrodeposition.

The samples with the conductive layer were degreased with ultrasounds in a mixture of acetone and ethanol for 5 minutes, to then be rinsed in distilled water and dried with blown air just before being coated.

The samples were then electrolytically coated through the potentiostatic method, and the deposition conditions were optimized at -0.75 V for 10 minutes by the use of an electrolyte with a composition of 0.005 M $ZnCl_2$ and 0.1 M KCl. A thermostatted bath was used for the cell at an optimum temperature of 75ºC. The cell assured the working conditions and sputtering in oxygen for a platinum

counter-electrode and a reference electrode of Ag/AgCl. These working conditions had been previously tested and optimized in the literature [11].

These working conditions allow homogeneous layers of ZnO to be obtained with the proper morphological characteristics for them to be used as an inorganic layer on the low-cost hybrid cells to be developed some time in the future on this basis.

3. EXPERIMENTAL CHARACTERISATION

3.1. SEM.

The ceramic material surface corresponds to a perfectly smooth and regular fired glaze coating. On to this surface, with an excessively smooth morphology, but which carries out its function as a barrier layer, an anchoring element has to be introduced for the electroless layer, which also increases the surface morphology to obtain a random by thermal spraying and the morphology is illustrated in the following figure:

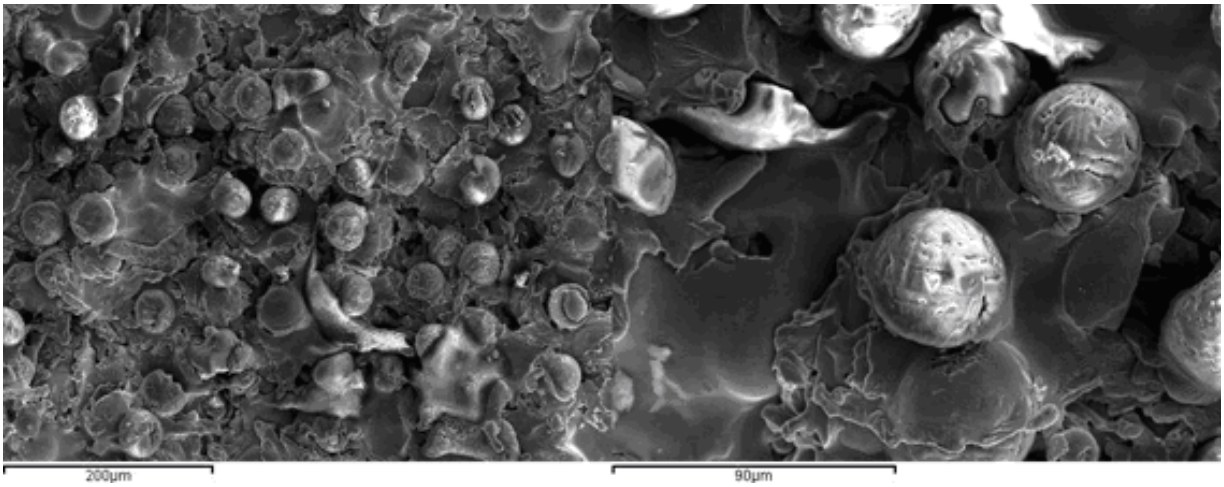

Figure 2. SEM images of the morphology of the thermally sprayed Ni layer.

The average size of the surface irregularities is around 30 µm, which represents a good compromise for the subsequent electrodeposition of ZnO [12]. The different polishing options then have to be carried out in order to adapt the completely random morphology to one with a better theoretical performance in electric properties. In the following images, the morphologies are compared after the different polishing options.

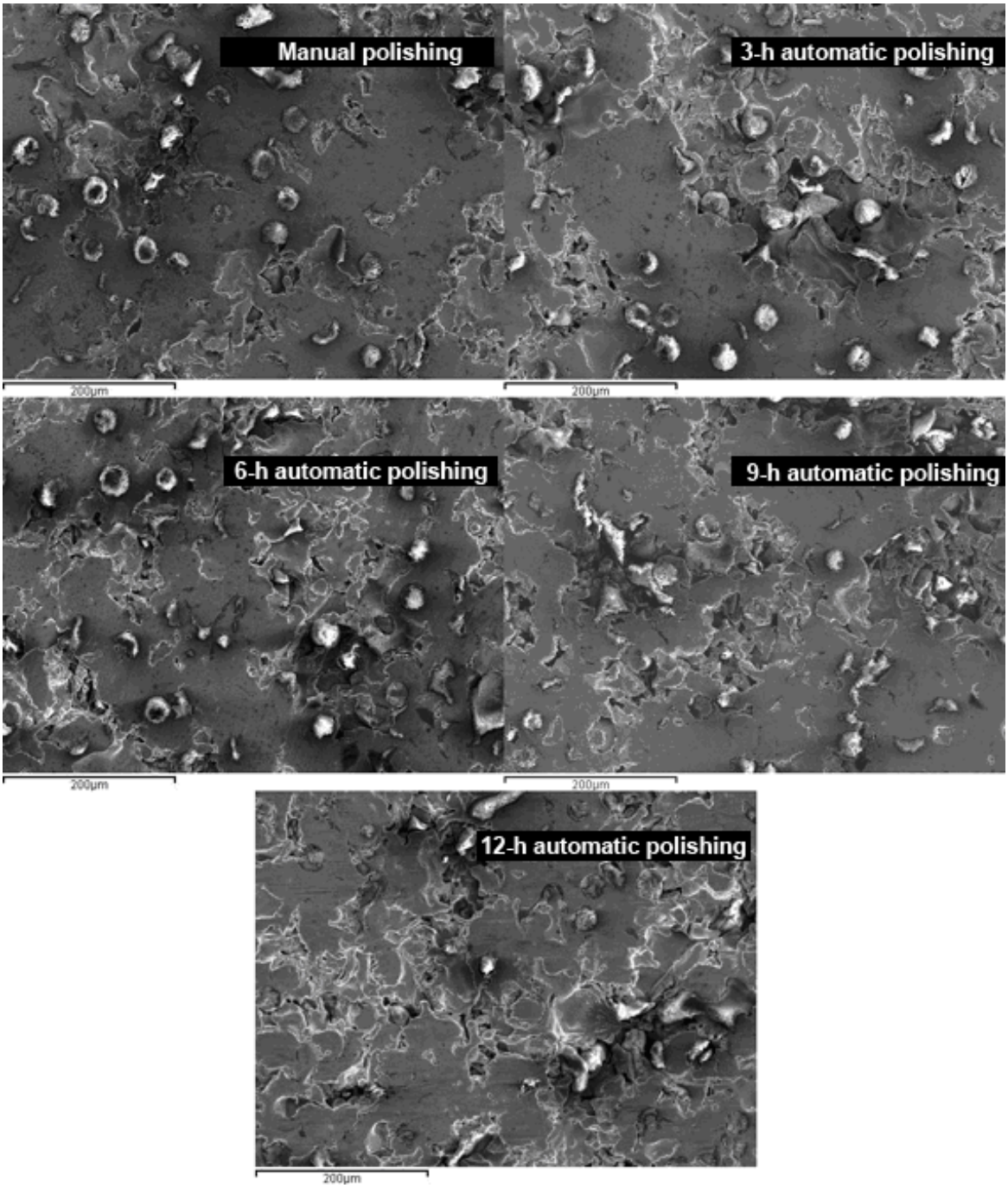

Figure 3. SEM images of the polished samples after thermal spraying.

The manually polished sample shows many irregularities and the flat area is estimated through image measurements at 32% of the total. The automatically polished samples display no irregularities (except the one polished for 12 hours, since at some points the entire sprayed layer has actually been eliminated) and the flat area percentages are 38% after 3 hours, 47% after 6 hours, 52% after 9 hours and 55% after 12 hours).

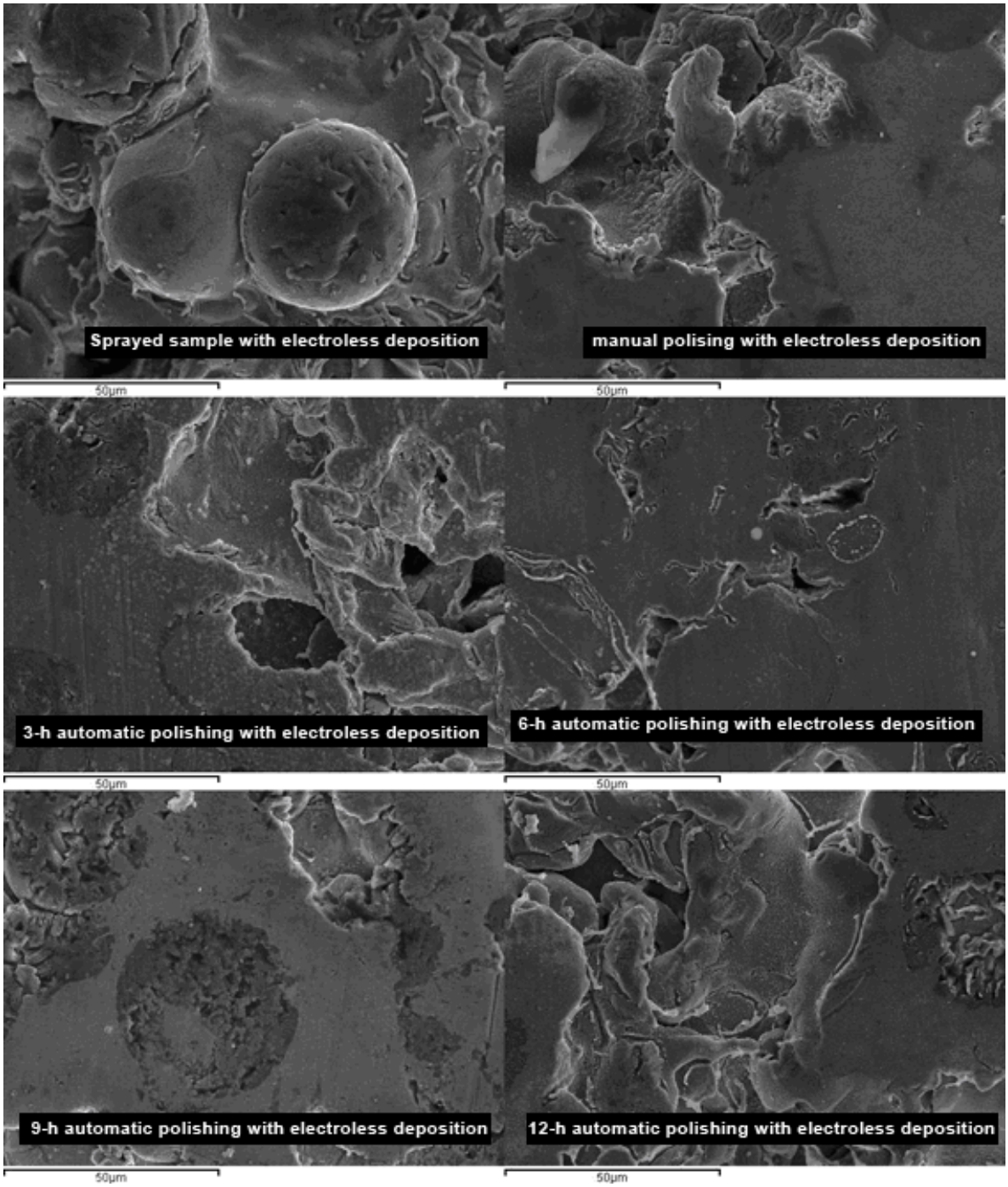

Figure 4. SEM images of samples with electroless deposition after polishing.

The typical electroless morphology of small lumps is shown both in the flat areas and in the hollows of the sprayed layer. In these interstices, there is less homogeneity of the texture. In all cases, the layer applied by electroless deposition is continuous and compact, although a loss of layer anchorage is detected in the sample automatically polished for 12 hours.

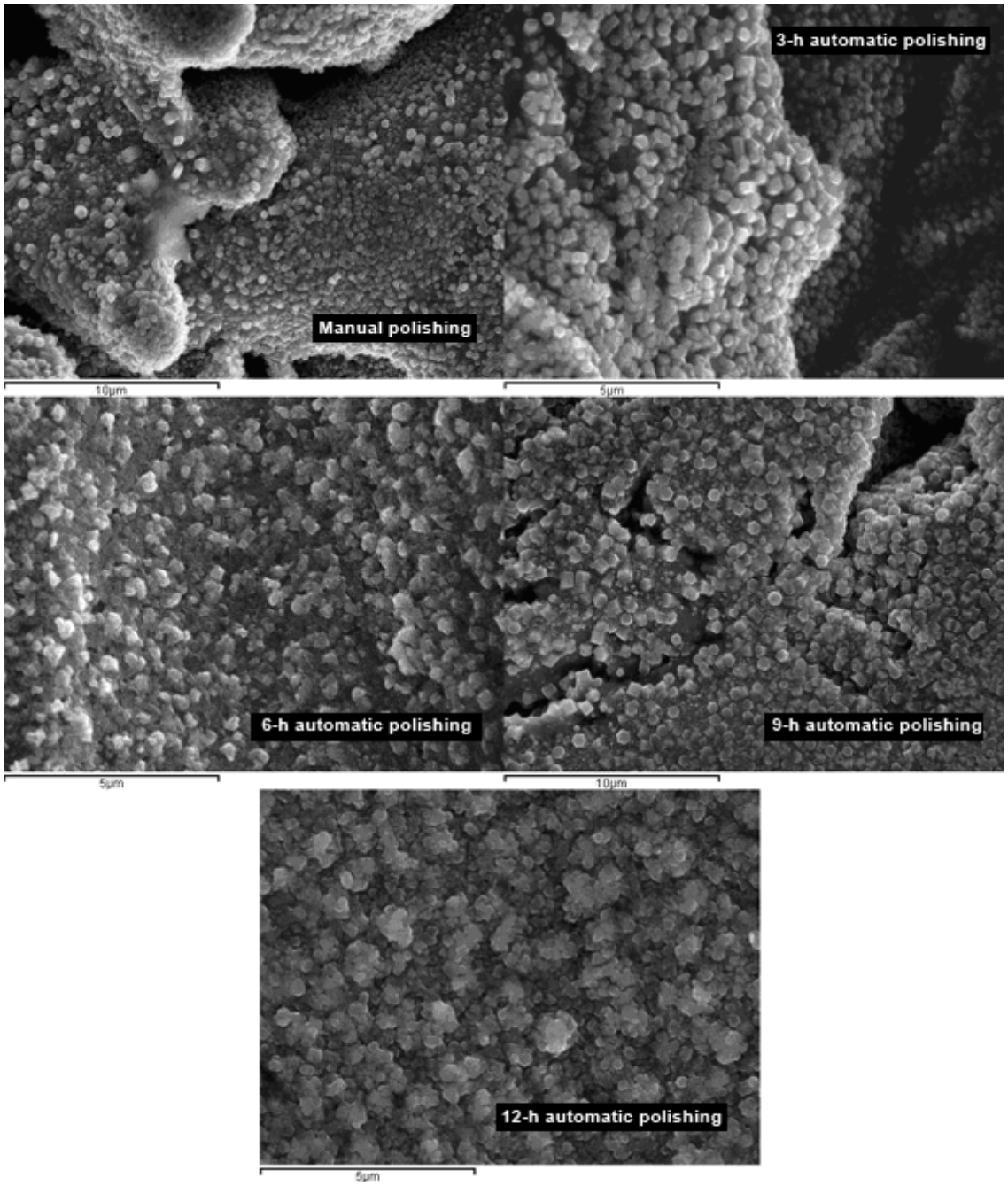

Figure 5. SEM images of the electrodeposited samples after electroless deposition.

In general, a high density of the electrodeposited wurtzite columns on the nickel is observed. The homogeneity of the sizes in the interstices decreases, as well as the uniform orientation. Lastly, it is concluded that in the flat areas there is more homogeneity, compactness and alignment of the columns. Consequently, the electric properties expected of the layers automatically polished for a longer time are better.

One effect that has not been quantified in this observation is the irregularities observed through fracture of the sprayed layer when the samples are polished for 12 hours.

3.2. AFM.

In order to quantify the roughness and morphology of the polished textures (with and without electroless deposition), a Veeco Multimode atomic force microscope (AFM) was used, with topography interpretation using the Nanoscope V5.30 r2 software: The samples were extracted by cutting with a diamond disc. Representative areas of 30 µm were analysed on the samples. An example of the topography on which the roughness analysis was carried out is shown below.

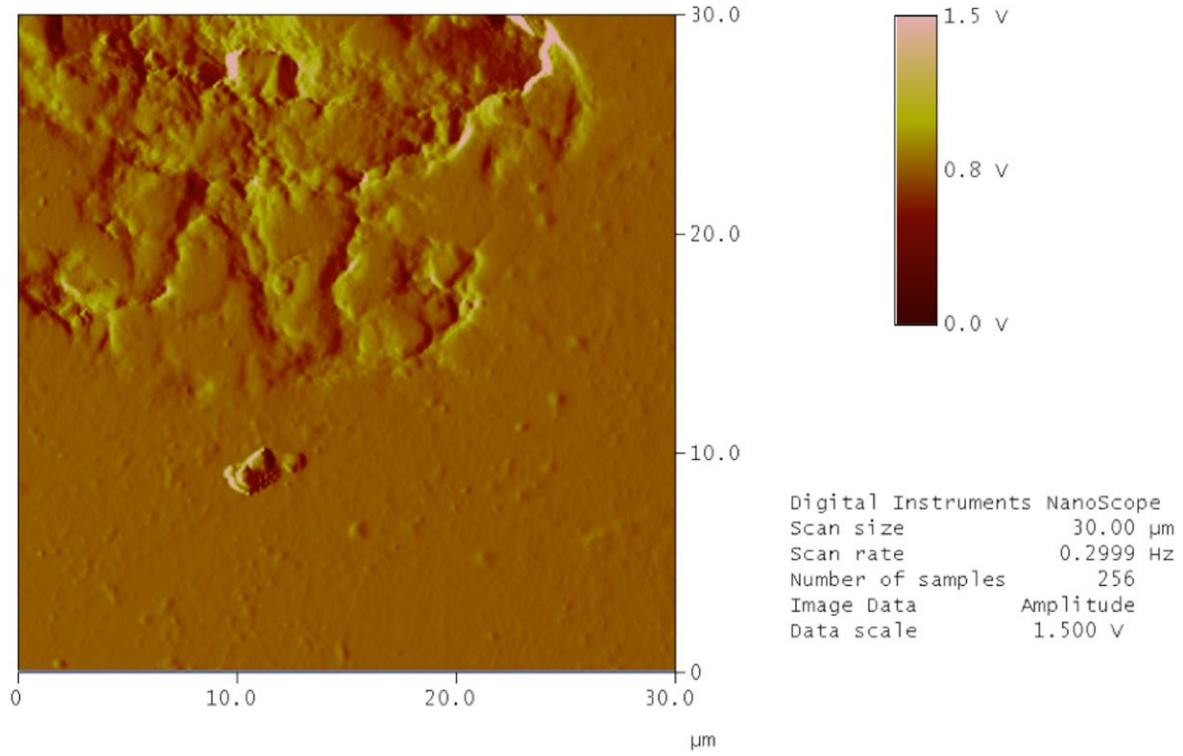

Figure 6. AFM topographic image of the manually polished sample.

The roughness analysis is intended quantitatively to compare the characteristics of the polishings obtained. In these circumstances, it is not necessary to calibrate the signal in millivolts in height in order to know its equivalent in length. The results of the main roughness parameters are shown in the following table.

State	Polishing	Rq (mV)	Ra (mV)	Rmax (mV)
Polishing	Manual	110.85	53.10	2270
	Automatic 3 hr	92.03	41.11	1900
	Automatic 6 hr	48.82	21.38	1740
	Automático 9 hr	23.85	14.32	817
	Automatic 12 hr	129.57	67.63	1862
Polishing + electroless deposition	Manual	66.77	37.27	1873
	Automatic 3 hr	85.63	35.74	1641
	Automatic 6 hr	40.86	27.57	1450
	Automatic 9 hr	25.87	26.98	2080
	Automatic 12 hr	85.12	46.03	2104

Table 1. Roughness analysis of the polished samples and with electroless deposition.

The results confirm that the electroless layer enhances the morphological conditions towards a smoother roughness. Additionally, after 9 hours' polishing, removal commences of the metal layer, which becomes quite pronounced after 12 hours' polishing.

Lastly, this analysis of the polished layers also verifies that the anchorage of the electroless deposition obtained by thermal spraying is adequate. Note that, perhaps, it might be better to increase the spray thicknesses in order to be able to perform more intensive polishing.

3.3. Corrosion.

Polarisation tests were carried out to study the corrosion behaviour of the metal layers formed according to the above polishing conditions. The polarisation curves are shown below, followed by their most characteristics parameters in table 2, to quantitatively assess their behaviour.

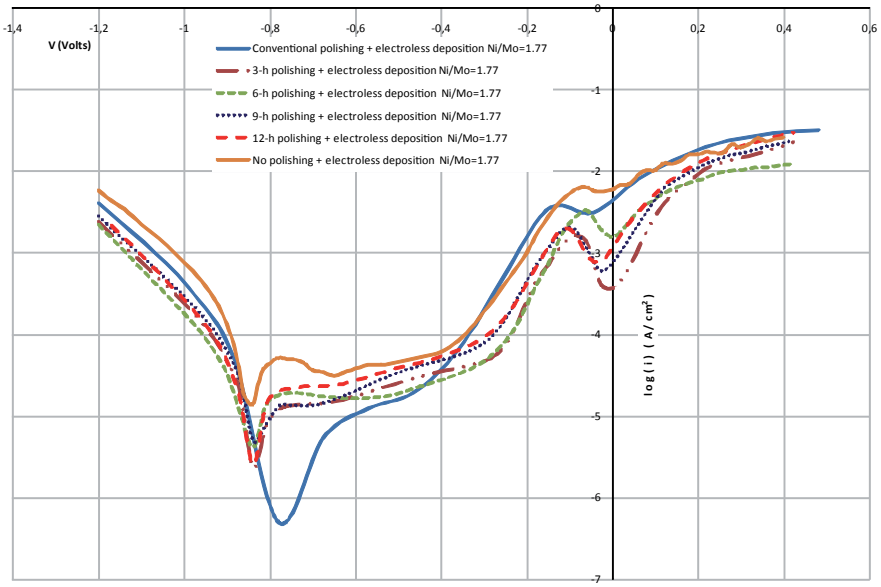

Figure 7. Polarisation curves of the samples after spraying, polishing (when appropriate), and electroless deposition.

	Electroless deposition Ni/Mo=1.77					
	Conventional polishing	3-h polishing	6-h polishing	9-h polishing	12-h polishing	No polishing
i_{corr} (amp/cm^2)	6.71E-06	9.16E-06	5.07E-06	1.01E-06	2.50E-06	5.00E-07
E_{corr}(v)	-0.675049	-0.809174	-0.839233	-0.809174	-0.839233	-0.840149
Tafel ba (v)	4.38E-02	0.0259027	-0.030694	0.066839	0.016590	7.06E-02
Tafel bc (v)	0.127872	0.0623096	0.025170	0.057609	0.014498	2.57E+01
Rp (Ω/cm^2)	2.11E+03	8.68E+02	1.20E+04	2.68E+01	1.34E+03	5.39E+02
B	0.014162	0.007945	0.060719	0.000208	0.003360	7.44E-03

Table 2. Results of the corrosion tests.

The results indicate that polishing impairs corrosion performance. The more intensive the polishing is, the higher the sensitisation. However, although the rise in corrosion with respect to the system without polishing is significant, there is still an adequate response which is better than in other typical systems [13].

3.4. Hall effect.

Measurements were made on the most significant electric characteristics of the ZnO layers using an instrument based on the Hall effect. The basic electric characterisation for determining the capacity of ZnO layers for forming part of the desired hybrid cells is shown in table 3.

Electric parameter	Without ZnO layer and without polishing	Polishing with ZnO layer			
		Manual	6 h	9 h	12 h
Concentration (1/cm^3)	-7.65E+20	2.56E+19	5.32E+21	2.18E+20	1.54E+20
Mobility (cm^2/Vs)	1.08E+02	3.83E+01	1.84E+01	7.25E+00	1.24E-03
Resistivity (Ω·cm)	7.57E-05	6.33E-04	6.37E-05	3.94E-04	3.27E+01
Magnetoresistance (Ω)	2.23E-03	2.92E-03	1.05E-03	1.29E-03	2.01E-03
Conductivity (1/Ω·cm)	1.32E+04	1.58E+03	1.57E+04	2.54E+03	3.06E-02

Tabla 3. Results of hall effect experiments.

In view of the results, polishing offers a significant improvement in the electric characteristics [5] and it is again seen that the appropriate polishing, for thermal spraying conditions, is 3-hour automatic polishing.

4. CONCLUSIONS

In view of the results set out, the real possibility of obtaining metal layers on ceramic substrates with good mechanical and corrosion characteristics is demonstrated. The ZnO layers display optimum electric characteristics for forming hybrid photovoltaic devices. The techniques used show the possibility of achieving a reasonable cost for industrial production of ceramic supports with direct incorporation into the construction and thereby of reducing the operating costs of solar use in buildings.

ACKNOWLEDGEMENTS

The authors wish to thank Professors Eric Kalu from Florida State University (USA) and Peter Kalu from the National High Magnetic Field Laboratory of Tallahassee (USA) for their collaboration, without which it would not have been possible to carry out this research. Finally, the authors gratefully acknowledge the collaboration of Ceramicas Belcaire (Roca Group), which provided the porcelain substrates on which the study was conducted.

REFERENCES

[1] Green, M.A.; Emery, K.; Prog. in Photovolt.: Res. and App.; Vol. 2, Issue 1 (2007) 27 – 34.

[2] Iencinella, D.; Centurioni, E.; Busana, M.G.; Solar Energy Mater. Solar Cells, 93, (2009) 206 – 210.

[3] Orozco-Messana, J.; Donderis, V,; Cembrero, J.; Hernández-Fenollosa, M.A.; Qualicer 2008, 95-102.

[4] Ni Dheasuna, C.; Mathewson, A.; Hecking, L.; Wrixon. G.T.;First WCPEC; Dec. 5-9, 1994; Hawaii, 1496-1499.

[5] Reyes-Tolosa, M.D.; Kalu, E.E.; Orozco-Messana, J.; Erb, A.; Kalu, P.N.; Hernández-Fenollosa, M.A.; Bolink, H.J.; 216th ECS Meeting, Vienna (2009) 57-69.

[6] Pawlowski, L.; Johm Wiley & sons (2008).

[7] Menner, R.; Gross, E.; Eicke, A.; Dittrich, H.; Springer, J.; Dimmler, B.; Rühle, U.; Kaiser, M.; Friedlmeier, T.; Schock, H.W.; Proceedings 13th European Photovoltaic Solar Energy Conference, Nice, France (1995), pp 2067-2071.

[8] Culha, O.; Celika, E.; Ak Azema, N.F.; Birlika, I.; Toparli, M.; Turk, A.; Journal of Materials Processing Technology, Vol. 204, Issues 1-3 (2008) 221-230.

[9] Kuruganti, A.S.; Chen, K.S.; Kalu, E.E.; Electrochemical and Solid-State Letters 2 (1) (1999) 27-29.

[10] Elsener, B.; Crobu, M.; Andrea Scorciapino, M.; Rossi, A.; Journal of Appl. Electrochem. (2008) 38:1053-1060.

[11] Donderis, V.; Orozco, J.; Cembrero, J.; Curiel-Esparza, J.; Damonte, L.C.; Hernández-Fenollosa, M.A.; Journal of Nanoscience and Nanotechnology Vol.10 (2010) 1-6.

[12] Baxter, J.B.; Aydil, E.S:; Solar Energy Materials & Solar Cells 90 (2006) 607–622.

[13] Lee, C.K.; Materials Chemistry and Physics 114 (2009) 125-133.